Chapter 20

Particulate Nanostructured Silicon Nitride and Titanium Nitride

R. A. Andrievski

Institute for New Chemical Problems, Russian Academy of Sciences, Chernogolovka, Moscow Region 142432, Russia

In recent years nanostructured (nanocrystalline, nanophase, or ultra-grained) materials (NM), which are commonly characterized by a grain size less than 100 nm, have attracted the most attention because of the hope of realizing the unique physical, mechanical, and chemical properties in the nanocrystalline state. In this connection the advanced ceramics as a whole, and silicon and titanium nitrides in particular because of their promising properties, are of great interest. Such properties of TiN and Si_3N_4 particulate NM as gas evolution at high-vacuum treatment and behavior during compaction, sintering, and high pressure sintering are described. The hardness values of these materials in the near dense state are discussed in detail. The necessity of further investigations is stressed.

Compared to the information for properties of some nanostructured metals (Cu, Ag, Ni, and Fe), intermetallics (TiAl and $NbAl_3$), and oxides (TiO_2 and ZrO_2), the data for high-melting compounds (nitrides, borides, and carbides) are very limited (*1-5*). It is common knowledge that silicon and titanium nitrides are the base of many tools and of structurally and functionally advanced materials. There is lot of information on properties of these nitrides in the conventional polycrystalline state and on single crystals (*6,7*). However, their investigation in the nanocrystalline state is only in beginning. Our selection of silicon and titanium nitrides was dictated not only by their practical applications but also by a desire to compare the behavior of compounds exhibiting different chemical bonding, i.e. covalent-ionic and metallic-ionic. We are focused only on particulate NM; thin film data will be shown for comparison.

Ultrafine Powders and Some of Their Characteristics

A large body of physical and chemical methods of preparation of high-melting compounds ultrafine powders (UFPs) has been examined in our papers(*4,5*). Thermal, plasma, and laser synthesis (decomposition), vaporization and condensation in

0097–6156/96/0622–0294$15.00/0

reactive gases, and mechanical synthesis, as applied to Si_3N_4 and TiN, are the processes used very extensively for obtaining UFPs. It should be noted that the main part of works performed in recent years concerns the silicon nitride gas-phase synthesis (*7*). Making possible homogeneous nuclei formation, to the greatest degree gas-phase synthesis is accompanied by UFPs preparation with particle size less than 100 nm (for the most part d<20 nm). Reactions between silicon tetrachloride vapor (or silane) and their derivations with ammonia conducted in plasma-chemical, laser-induced or conven-tional thermal interactions were the subject of many investigations (see, for example Refs.(*8-13*)). The conditions of the thermal and laser pyrolysis of the crosslinked organosilicon polymers have also been analyzed in detail as applied to different gases (argon, oxygen, nitrogen, and helium) (*14,15*). Use of NMR and FTIR spectroscopy helped in the identification of different intermediate compounds formed. Plasma methods of UFPs preparation , fixed in to some extent as traditional, do not lose their importance (*9,10,16,17*) while using laser synthesis method is unique to the laboratory scale. Meanwhile, works for using gas-phase reactions in conditions of flowing thermal reactors are extending both for Si_3N_4 and TiN (*13,18,19*; Winter, G., H.C.Starck Co., personal communication, 1995).

Properties of Si_3N_4 and TiN UFP have been analyzed elsewhere (*4,5,7,20*). The most interesting features are the great enrichment of the particle surface in oxygen, carbon, and other admixtures and the poor compressibility of UFPs. According to data (*21*) the oxygen and carbon presence in surface layers of different Si_3N_4 UFPs is respectively 2-20 and 10^2-10^3 times higher than the bulk content. It is also interesting that there was no correlation between the overall chemical composition and the particle size of the powders in the experimental range of d values. The enrichment of the surface layers in oxygen and carbon was likewise weakly correlated with overall content of these impurities. It is also worthy of note that there are many other results which confirm the surface enrichment of TiN and Si_3N_4 UFPs in oxygen and carbon (for example, data obtained by XPS and AES methods (*5,7*)). Whereas the increased content of oxygen on the surface can be naturally attributed to oxidation, in order to elucidate the causes of the enrichment in carbon it is useful to turn to the results of the study of gas evolution during the high-vacuum heat treatment of UFPs.

Figure 1 shows the influence of the high-vacuum treatment temperature on the rate of gas evolution for TiN UFP (d~70 nm) (5). One can see that there are two gas evolution peaks at ~250°C (for H_2O and N_2) and at ~650°C (for CO,CO_2 , and H_2). Carbon monoxide dominates appreciably in the evolving gases. XPS study has also revealed the enrichment of the surface layers in oxygen and carbon-containing components. A similar situation has also been observed in the case of Si_3N_4 UFP (*7*). Table I shows the content of evolved gases for amorphous plasma Si_3N_4 powders (d~20 nm) during high-vacuum heat treatment. Temperatures of maximum rate of gas evolution for CO, H_2, and N_2 were 500-900°C and for H_2O and CO_2 ones were 300-400°C. Vacuum annealing results in significant decreasing desorbed gas quantity; however, the whole picture remains valid. It should be noted that it is not clear why the dominant species in the desorbed gas below 1000°C is carbon monoxide, and not carbon dioxide, as could have been expected from the well known equilibrium of the Bell-Boudouard reaction. To gain a better understanding into this mechanism further investigations using different methods are badly needed.

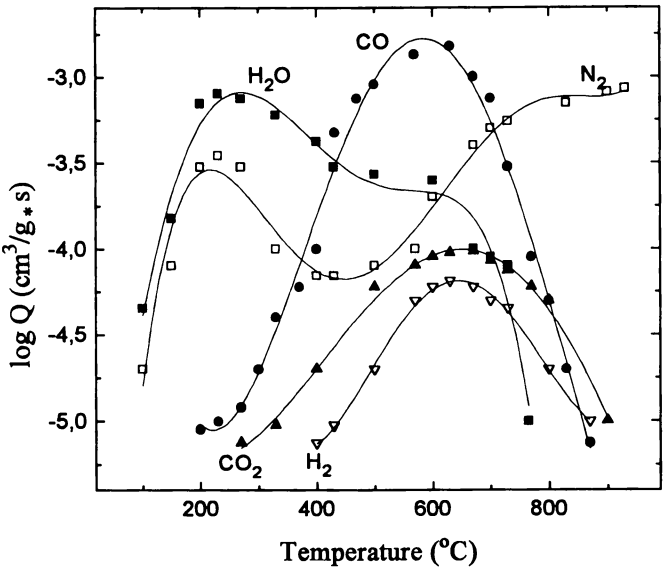

Figure 1. Temperature dependence of the rate of gas evolution Q for TiN UFP

Table I. Some Parameters of the Gas Evolution for Si_3N_4 UFP before (1) and after High-Vacuum Annealing for 1 h at 1200°C (2)

Powder type	*Total gas volume* (cm^3/g)	*Predominant gas content (mass%)*			
		CO	H_2	N_2	H_2O
initial (1)	625	59	11	21	9
annealed (2)	89	79	7	10	4

Another interesting feature of UFPs is their behaviour at compaction. It is well known that the compressibility of powders decreases markedly with decreasing particle size and so the UFPs compressibility is very poor. The last may be connected with severe interparticle friction of powders with high value of specific surface area. Beside that the poor ductility characteristics of TiN and especially Si_3N_4 are also responsible for the low compressibility of their powders. However, regarding UFPs the main factor determining compressibility is interparticle friction. As it was stressed in our paper (*20*) the compressibility of ductile nickel powder and brittle silicon nitride is nearly similar in the ultradispersed state. Table II demonstrates the comparison of the compressibility of silicon and titanium nitrides as well as nickel UFPs (*4,5,20*).

Table II. Influence of Particle size (*d*) and Compaction Pressure (*P*) on Relative Density of Si_3N_4, TiN, and Nickel UFPs (the Compact Diameter of ~10 mm)

Powder	*d(nm)*	*Relative Density at P (GPa)*			
		1	*4*	*6*	*8*
	1000	0.64	0.74	0.79	0.82
Si_3N_4	50	0.54	0.65	0.7	0.72
	17	0.47	0.55	0.58	0.62
TiN	80	0.64	0.8	0.84	0.85
	70	0.6	0.75	0.8	0.81
Ni	50	0.58	—	—	—
	15	0.49	—	—	—

From these data it is evident that the behavior of these powders during compaction seems to be roughly similar; however, the influence of pressure on relative density is more evident in the case of TiN. This can be explained by more covalent and respectively more brittle nature of silicon nitride. It has been pointed out that there is significant influence of chemical bond on compressibility for UFPs. It is also important to indicate that there is no possibility to obtain near dense compacts from UFPs in the conditions of cold compaction even at the compaction pressures up to 8-9 GPa.

NM Consolidation and Properties

One of the main problems in NM processing is consolidation with full densification and without sacrificing their nanocrystalline structure. Methods of UFPs consolidation, such as compaction and sintering, hot pressing, hot forging, shock compaction, electro-discharge compaction, high pressures and high temperatures technique, etc., have been discussed in review (*4*). Typical densification S-curves at pressureless sintering have been demonstrated in particular for metallic, metal-similar (like TiN), and covalent (like Si_3N_4) solids. The marked difference in the temperatures of active and full densification for metallic, metal-similar, and ionic solids, on the one hand, and for covalent ones, on the other was very striking. In first case, the sintering temperature of UFPs is substantially below that for conventional powders and ranges from 0.3 to $0.5T_m$ (T_m is melting point). However, for covalent solids (boron, silicon, Si_3N_4, etc.) the estimated active densification temperature during sintering is about 0.85 T_m or higher. Si_3N_4 powders, even UFPs, are very difficult to densify without sintering aid, which is connected with the covalent origin of Si_3N_4 and its low diffusion and dislocation mobility.

For the most part intensive recrystallization accompanies high-temperature sintering obligatory and in these conditions the nanocrystalline structure disappearance is

very likely. So only high-energy consolidation methods, such as shock compaction, high pressure and high temperature technique, etc., seem to be useful for effective NM processing. As applied to TiN and Si_3N_4 materials such experimental data are not comprehensive.

In our experiments with Si_3N_4 UFP (*4,7,20*), it was shown that increasing the compaction pressure from 1.5 GPa to 8.5 GPa results in a significant decrease of the densification temperature from ~1900°C to ~1100°C. The grain size of Si_3N_4 UFP compacted at 1200°C (P=8.5 GPa) was 0.5-1 μm (the initial particle size was ~50 nm). Shock-compacted Si_3N_4 powder was characterized by the grain size of 40-60 nm. In these experiments the compaction pressure and estimated temperature were respectively 40 GPa and 1200 K (*22*).

Figure 2 shows the change of relative density, hardness, and elastic modulus during pressure sintering of TiN UFP; the data for pressureless sintering are also demonstrating for comparison (*23*; Andrievski, R.A.; Urbanovich, V.S.; Kobelev, N.P.; Kuchinski, V.M. *Proc. IV European Ceramic Society,* Riccione, 2-5 October, 1995, in press). One can see that using the compaction pressure of 4 GPa results in a decrease of the active densification temperature on 600-800°C. It is also evident that the further pressure increase is not so effective. As is also clear from Figure 2, the elastic modulus and the hardness of specimens are practically changed monotonously as a density. As applied to the elastic modulus values obtained data seemed to be near those for the dense specimens (435-440 GPa) and some difference can be attributed to porosity influence. Some residual porosity of 1-3% was present in our near dense specimens. The fact that the hardness values were not changed in the interval from 1130°C to 1400°C may be explained in conjunction with the possible contribution between the porosity decrease and the recrystallization progress.

The XRD study has revealed only one phase of TiN in high-pressure sintered specimens. It was also detected that after heat and pressure treatment (T=1130-1200°C, P=4 GPa) the crystallite size and the magnitude of internal stresses derived from (422) line-broadening were 65-75 nm and $(2.2\text{-}2.7)10^{-3}$ respectively. The preliminary TEM observation of the specimen obtained at 1000°C (P=4 GPa) has revealed two kinds of crystallites with the sizes of 50-100 nm and of ~700 nm respectively. No additional phases were detected at the grain boundaries and triple junctions. At the same time, the optical microscopic and SEM study has revealed the inclusions presence. Their size varied from about micrometer parts to some micrometers but the main part had the size of 2-5 μm. The SEM investigations of fracture surfaces have also revealed the heterogeneous character of fracture. In some places of specimens the transgranular one has been observed. However, in many places the elucidation of structural peculiarities of fracture demands the more high resolution of SEM in comparison with our disposal. The inclusions hardness was lower than one for the main phase and was equal to 10-20 GPa. The largest inclusions had the least hardness value. The inclusions presence in the high pressure sintered specimens can be attributed both to their presence in initial UFP and to the result of beginning dynamic recrystallization. The detailed analysis of microstructure has been carried out elsewhere (Andrievski, R.A. *Proc.6th Int.Symp. Fract.Mech.Ceram.*, Karlsruhe, 18-20 July, 1995).

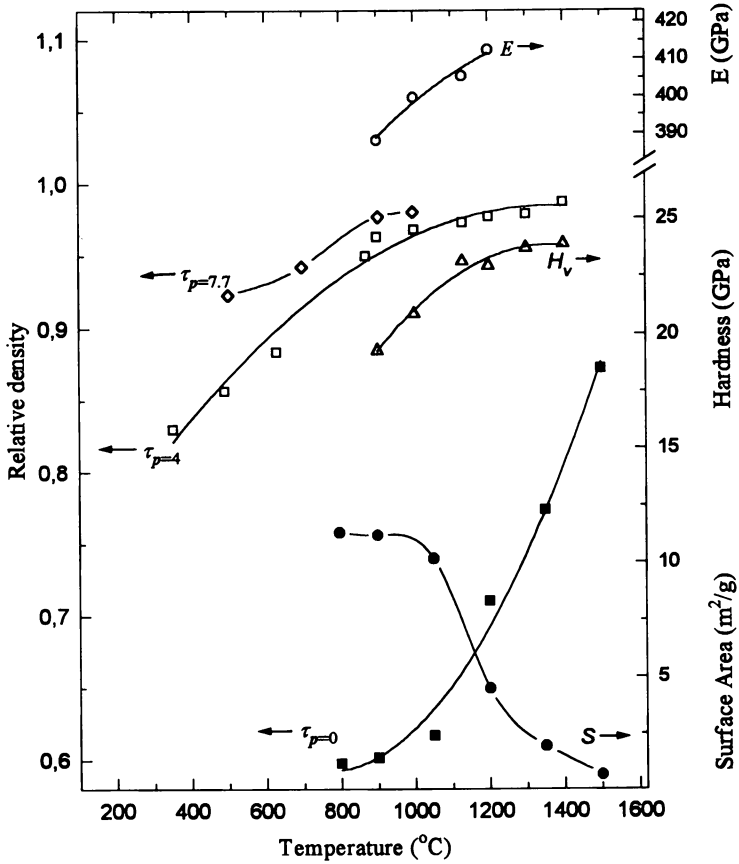

Figure 2. Effect of temperature on relative density (τ_p), microhardness (H_v), elastic modulus (E) at P=4 GPa and τ_p at P=7.7 GPa as well as on $\tau_{p=0}$ and specific surface area (S) during pressureless sintering.

It seems to be important to compare our densification and hardness data with literature information for TiN and Si_3N_4 materials. Table III summarizes this information. First of all it should be particularly emphasized that because of the different processing time, the distinct H_v and L measurements methods, etc., it is not easy to compare all these results. Some discrepancy is evident both for TiN and Si_3N_4. In the last case the enough modest results (*22*) may be connected with the low processing temperature. At the same time, however, it should be noted that mostly our H_v data for TiN are higher than those for the conventional sintered or hot-pressed materials which is likely connected with the presence of the nanocrystalline structure in our specimens.

Table III. Preparation Conditions and Some Properties of Near Dense TiN and Si_3N_4 Materials

Powder	*d*[a] *(nm)*	*T(°C)*	*P(GPa)*	*τ*	*L*[b] *(nm)*	H_v *(GPa)*	*Source*
TiN	~40	1500	0.04	0.96	$\sim 10^4$	20-23	(*24*)
TiN	$\sim 10^3$	2100	0.14	0.94	$\sim 10^4$	10-11	(*25*)
TiN	~40	1300	–	0.99	~200	10	(*26*)
TiN	500-2 10^3	1850	0.03	0.94	2.5 10^3	12	(*27*)
TiN	~80	1100	4	0.98	65-75	24	(*23*)
Si_3N_4	~50	1200	8.5	0.99	500-10^3	32.4	(*5*)
Si_3N_4	~70	900	40	0.99	40-60	22	(*22*)

[a] *d* - the initial mean particles size.
[b] *L* - the specimens mean grain size.

It is also interesting to compare obtained results with ones for TiN films and Si_3N_4 single crystals. To our knowledge (*4,5*) the highest hardness values for TiN films are 45-75 GPa including data for nanocrystalline films (*L*~20 nm) and superlattice and multilayer ones (*L*~5-10 nm). The maximum hardness values of Si_3N_4 single crystal are also very high (up to 35-45 GPa) (*6,7*); at the same time, for monolithic polycrystalline Si_3N_4 microhardness is about 20-25 GPa (*6*). So our results are higher than those for the conventional dense polycrystalline TiN and Si_3N_4 specimens, however, they are smaller in comparison with TiN nanocrystalline films and Si_3N_4 single crystals. Therefore, the further investigations of the TiN and Si_3N_4 materials with the grain size of 10-20 nm seem to be very desirable.

Conclusions

To sum up this examination, it can been seen from the foregoing that only first steps have been taken in the study of silicon and titanium nitrides in the nanocrystalline state. The almost similar situation is in the case of another high-melting ceramic compounds. Problems, such as the selection of optimal UFPs preparation and conso-lidation methods in term of NM quality and cost effectiveness, the role of admixture, the origin of hardness and its relationship with grain size, nanophase equilibria in the systems $Ti–N_2$, $Si–N_2$, etc., and many others, remain unresolved and need further consideration and clarification.

Acknowledgments

The results described in this paper was made possible in part by the grants from the International Science Foundation and the Russian Government (NoMTF 300) and the Russian Basic Research Foundation (No 95-02-0318a).

I am sincerely grateful to Drs.G.V.Kalinnikov, M.A.Leontiev, R.A.Luitikov, and V.S.Urbanovich for their active assistance in this investigation.

Literature Cited

1. Gleiter, H. *Nanostr.Mater.* **1995,** *6,* 3.
2. Siegel, R. *Nanostr.Mater.* **1994,** *4,* 121.
3. Suryanarayana, C. *Int.Mater.Rev.* **1995,** *40,* 41.
4. Andrievski, R.A. *J.Mater.Sci.* **1994,** *29,* 614.
5. Andrievski, R.A. *Russ.Chem.Rev.* **1994,** *63,* 411.
6. Andrievski, R.A.; Spivak, I.I. *Strength of High-Melting Compounds and Materials on Their Base (in Russ.);* Metallurgia: Cheliabinsk, **1989;** pp.201-229.
7. Andrievski, R.A. *Russ.Chem.Rev.* **1995,** *64,* 291.
8. Lange, H.; Wotting, G.; Winter, G. *Angew.Chem.* **1991,** *30,* 1579.
9. Lee, H.J.; Eguchi, K.; Yoshida, T. *J.Am.Ceram.Soc.* **1990,** *73,* 3356.
10. Allaire, F.; Dallaire, S. *J.Mater.Sci.* **1991,** *26,* 6736.
11. Bauer, R.A.; Becht, J.G.M.; Kruis, F.F.; Scarlet, B., Schoonman, J. *J.Am.Ceram. Soc.* **1991,** *74,* 2759.
12. Danforth, S.C. *Nanostr.Mater.* **1992,** *1,* 197.
13. Chang, W.; Skadan, G.; Danforth, S.C.; Kear, B.H. *Nanostr.Mater.* **1994,** *4,* 507.
14. Gonsalves, K.E.; Strutt, P.R.; Xiao, T.D. *J.Mater.Sci.* **1992,** *27,* 3231.
15. Bahlout, D.; Pereira, M.; Goursat, P.; Choing Kwet Yive, N.S.; Corriu, R.J.B. *J.Am.Ceram.Soc.* **1993,** *76,* 1156.
16. Heidemane, G.M.; Grabis, Ja.P.; Miller, T.N. *Izv.Akad.Nauk SSSR. Neorg.Mater. (in Russ.)* **1979,** *15,* 596.
17. Batenin, V.M.; Klimovski, I.I.; Lysov, G.V.; Troitskii, V.N. *Superhigh Frequency Generators of Plasma;* CRS Press: Boca Raton, **1994;** pp.172-212.
18. Rabe, T.; Wasche, R. *Nanostr.Mater.* **1995,** *6,* 357.
19. Deccer, J.P.; van der Put, P.J.; Veringa, H.J.; Schoonman, J. *J.Mater.Chem.* **1994,** *4,* 689.
20. Andrievski, R.A. *Int.J.Powd.Metall.* **1994,** *30,* 59.
21. Szepvolgyi, J.; Bertoti, I.; Mohai-Toth, I.; Gilbart, E.; Riley, F.L.; Patel, M. *J.Mater.Chem.* **1993,** *3,* 279.
22. Hirai, H.; Kondo, K. *J.Am.Ceram.Soc.* **1994,** *77,* 487.
23. Andrievski, R.A.; Kalinnikov, G.V.; Potafeev, A.F.; Urbanovich, V.S. *Nanostr. Mater.* **1995,** *6,* 353.
24. Torbov, V.I.; Troitskii, V.N.; Rakhmatullina, A.Z. *Powd.Metal.(in Russ.)* **1979,** (*No12*), 28.
25. Moriyama, M; Komata, K.; Kobayashi, Y. *J.Cer.Soc.Jap.* **1991,** *99,* 286.
26. Ogino, Y.; Miki, M.; Yamasaki, T.; Inuma, T. *Mater.Sci.Forum* **1990,** *88-90,* 795.
27. Graziani, T.; Melaudri, C.; Bellosi, A. *J.Hard Mater.* **1993,** *4,* 29.

RECEIVED January 25, 1996